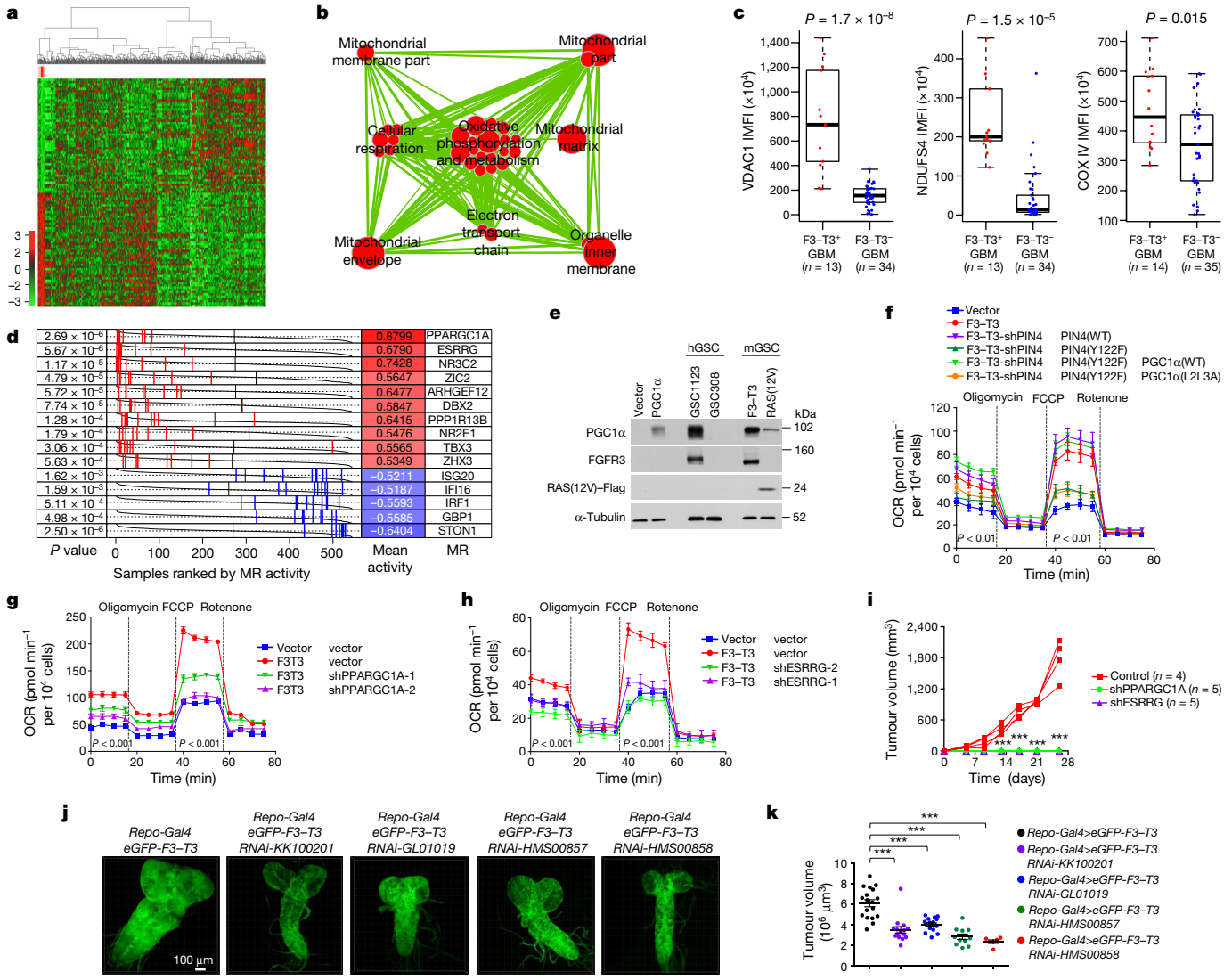

Figure 3 | PGC1α and ERRγ are required for F3–T3-mediated mitochondrial metabolism and tumorigenesis. a, Hierarchical clustering of GBM ($n = 534$) and normal brain ($n = 10$) from the TCGA using DEGs in nine F3–T3-positive samples (red) versus the F3-T3-negative samples. **b**, Enrichment map network of statistically significant GO categories in nine F3–T3-positive samples (upper-tailed MWW-GST $Q < 0.001$, normalized enrichment score (NES) > 0.6). Nodes represent GO terms and lines their connectivity. Node size is proportional to number of genes in the GO category and line thickness indicates the fraction of genes shared between groups. **c**, Quantification of IMFI of VDAC1, NDUFS4 and COXIV in F3–T3-positive and F3–T3-negative GBM. Box plot spans the first to third quartiles and whiskers show the 1.5× interquartile range. $P \leq 0.0001$ (VDAC and NDUFS4); $P \leq 0.05$ (COXIV), two-sided MWW test. **d**, Master regulator (MR) activity in GBM. Grey curves represent the activity of each master regulator. Red or blue lines indicate individual F3-T3-positive GBM displaying high or low master regulator activity, respectively ($n = 534$). *P* value, two-sided MWW test for differential activity (left) and mean of the activity (right) of the master regulator in F3–T3-positive versus F3–T3-negative samples are indicated. **e**, Immunoblot of PGC1α, in human (h) and mouse (m)GSCs. Human astrocytes transduced with PGC1α or vector are controls. **f**, OCR of F3–T3 human astrocytes following silencing of *PIN4* and reconstitution with PIN4(WT) or PIN4(Y122F), in the presence or the absence of PGC1α(WT) or PGC1α(L2L3A). **g**, OCR of F3–T3 human astrocytes transduced with *PPARGC1A* shRNA. **h**, OCR of F3–T3 human astrocytes transduced with shESRRG. **i**, Tumour growth of F3–T3 human astrocytes transduced with vector ($n = 4$), *PPARGC1A* shRNA1 ($n = 5$) or *ESRRG* shRNA1 ($n = 5$). Tumour growth curves of individual mice are shown. **j**, Representative images of whole brain–ventral nerve cord complex optical projections from *repo-Gal4>F3–T3* and *repo-Gal4>F3–T3* with *srl* RNAi *Drosophila* larvae. **k**, Quantification of tumour volume of *repo-Gal4>F3–T3* and repo-Gal4>F3–T3 with *srl* RNAi *Drosophila* larvae. **f**–**h**, Data (mean ± s.d.) are from two experiments (**f**, $n = 3$ and $n = 5$ technical replicates, respectively, per experiment) or one (**g**, **h**, $n = 4$ technical replicates) experiment. **k**, Data are mean ± s.e.m. ($n = 6$–17 larvae) of one experiment. Experiments were repeated two to three times with similar results. $^{**}P \leq 0.01$, $^{***}P \leq 0.001$, two-tailed *t*-test with unequal variance (**f**–**k**).

F3–T3-mediated induction of PGC1α (Extended Data Fig. 7a, c). The inhibition of mitochondrial metabolism and reduction in soft agar clonogenicity by PIN4(Y122F) in F3–T3 human astrocytes were both rescued by overexpression of PGC1α(WT). Conversely, PGC1α(L2L3A), which contains mutations in the nuclear receptor boxes L2 and L3 that are critical for binding ERRγ[18] could not rescue F3–T3-mediated activation of mitochondrial metabolism in F3–T3 human astrocytes expressing PIN4(Y122F) (Fig. 3f and Extended Data Fig. 7e, f). Finally, loss of PGC1α by shRNA and CRISPR–Cas9 gene editing reversed the activation of mitochondrial respiration by F3–T3 and depletion of ERRγ produced similar effects (Fig. 3g, h and Extended Data Fig. 7g–m). PGC1α silencing inhibited soft agar colony formation by F3–T3 human astrocytes and impaired self-renewal of GSC1123 cells (Extended Data Fig. 7n–p). Silencing of either *PPARGC1A* or *ESRRG* prevented tumour xenograft formation of F3–T3 human astrocytes in mice (Fig. 3i and Extended Data